Journal of Applied Polymer Science

Iron Chelating Polypropylene Films: Manipulating Photoinitiated Graft Polymerization to Tailor Chelating Activity

Maxine J. Roman, Fang Tian, Eric A. Decker, Julie M. Goddard
Department of Food Science, University of Massachusetts, Amherst Massachusetts 01003
Correspondence to: J. M. Goddard (E-mail: goddard@foodsci.umass.edu)

ABSTRACT: Transition metals, especially iron, enhance the oxidative degradation of lipids. Nonmigratory metal chelating active packaging can inhibit lipid oxidation and meet consumer demand for 'cleaner' labels. Recently, the development of iron chelating films prepared by photoinitiated graft polymerization of acrylic acid on polypropylene (PP-*g*-PAA) was reported. The objective of this study was to tailor the chelating activity of PP-*g*-PAA by manipulating graft conditions. Carboxylic acids graft density and PAA graft thickness increased with graft time and acrylic acid concentration, with carboxylic acids density of up to 143 ± 32 nmol cm^{-2}, PAA graft thickness of ~6–18 μm, and ligand (carboxylic acid) to metal (Fe^{2+}) binding ratio of ~4–5. Reducing photoinitiator graft density decreased this ratio to ~2–2.5, suggesting that graft chain density influences chelating activity. This work demonstrates the ability to tailor chelating activity of PP-*g*-PAA with potential applications in active packaging, chelation therapy, and water purification. © 2013 Wiley Periodicals, Inc. J. Appl. Polym. Sci. **2014**, *131*, 39948.

KEYWORDS: grafting; packaging; photopolymerization; polyolefins; metal chelators

Received 29 July 2013; accepted 8 September 2013
DOI: 10.1002/app.39948

INTRODUCTION

The presence of trace amounts of transition metals, especially iron, promotes deterioration of food quality via lipid oxidation. Metal-promoted lipid oxidation is primarily initiated by the reduced state of iron, ferrous iron (Fe^{2+}), which reacts with hydroperoxides to create radicals that propagate oxidation and contribute to the formation of off flavors, loss of nutrients, and degradation of color.[1] Since it is difficult to completely remove trace amounts of iron from foods and the processing environment, the principal method of inhibiting metal-promoted lipid oxidation is the addition of metal chelators that bind iron to hinder its reactivity.[2] The most effective (and most widely used) metal chelator is a synthetic compound ethylenediaminetetraacetic acid (EDTA). In an effort to produce foods with less synthetic additives, there has been increasing interest in alternative methods of inhibiting metal-promoted lipid oxidation. These methods include the replacement of synthetic additives with natural antioxidants and/or active packaging. Natural antioxidants tend to be less potent than their synthetic counterparts and therefore must be added to food products in excessive quantities that have yet to be evaluated for safety and may have adverse impacts on sensory perception.[3] Active packaging is a promising area of research that investigates the incorporation of active compounds, such as antioxidants, into the food packaging rather than directly into the food product.[4] However, most of the research in this area has been dedicated to the development of active packaging where functionality relies on the migration of active compounds from the packaging into the food, thus requiring labeling as an additive. Recently, nonmigratory iron chelating active packaging was developed with the intended use of inhibiting lipid oxidation in liquid and semiliquid foods.[5,6] Compared with traditional active packaging, in which the active agent would require approval as a *direct additive*, the active agent in nonmigratory active packaging would require *food contact notification*.[7]

Nonmigratory active packaging can be synthesized by direct covalent binding or tethering of active compounds to the surface of common packaging materials.[8,9] This concept has been used to modify surfaces for immobilization of enzymes and inhibition of microbial growth.[10–12] To bind active compounds to packaging, their inert surfaces must be pretreated to create active sites. Some techniques for surface activation include wet chemical, silanization, ionized gas treatments (i.e., plasma, corona discharge, and flame treatment), and UV irradiation.[8,13–16] UV radiation is a low cost and easy to control method that yields uniform, high density surface modifications with minimal damage to bulk material properties, which makes it advantageous compared to other surface modification techniques.[15]

Additional Supporting Information may be found in the online version of this article.

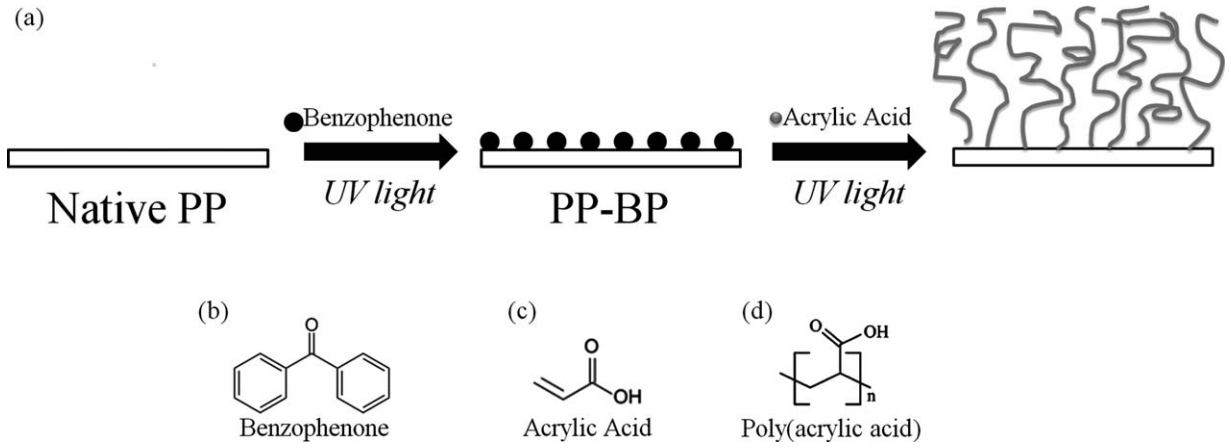

Figure 1. Two step photoinitiated graft polymerization of acrylic acid onto polypropylene—PP-*g*-PAA (a) and the chemical structures of (b) photoinitiator, (c) monomer, and (d) grafted polymer.

The current generation of iron chelating active packaging relies on the chelating activity of polymers covalently bound to the surface of films by photoinitiated living graft polymerization.[6] The basic principle of photoinitiated living graft polymerization relies on using a photoinitiator in the presence of UV light to abstract a hydrogen to create surface radicals that can bind the photoinitiator to the film's surface.[17,18] Then, a vinyl or acrylic monomer in the presence of UV light replaces the photoinitiator and polymerizes onto the surface to form polymer chains. Extensive research on photoinitiated graft polymerization of acrylic acid has been conducted in the field of membrane technology for the purpose of reducing protein fouling and tailoring membrane permeability. Successful grafting of poly (acrylic acid) to polypropylene (PP),[17,19–23] polyamide,[23,24] polyethersulfone,[25,26] cellulose acetate,[22] and polyvinylidene fluoride[22] membranes by photoinitiated graft polymerization has been previously reported. Poly(acrylic acid) surface grafts onto polyolefin films, such as polyethylene[27] and PP,[28,29] have been shown to reduce gas permeability.

The iron chelating activity of poly(acrylic acid) chains bound to polypropylene films (PP-*g*-PAA) by photoinitiated graft polymerization has been demonstrated.[6] A basic schematic of this surface modification method is shown in Figure 1. This surface modification utilizes a sequential surface application of the photoinitiator and the monomer, which allows for controlled grafting of polymer chains with minimal homopolymer and crosslinking reactions.[17] The active functional group on acrylic acid that binds metal ions is carboxylic acid. Carboxylic acids are found in many common food grade chelators, including EDTA and citric acid.[4] The theoretical ligand (carboxylic acid) to metal (Fe^{2+}) binding ratio of poly(acrylic acid) chains is 2 as depicted in Figure 2. This ratio may be observed to be different experimentally due to steric restriction of polymer grafting and/or environmental conditions (i.e., pH and ionic strength). It was previously reported that PP-*g*-PAA extended the lag phase of lipid oxidation in a soybean oil-in-water emulsion from 2 to 9 days compared with native PP.[6]

Inhibiting metal-promoted oxidative degradation by such non-migratory iron chelating films has application in an array of food, beverage, and consumer products applications, however individual applications may have different chelation needs as determined by factors such as iron concentration, pH and ionic strength. As such, it is important to optimize photoinitiated graft polymerization to tailor its iron chelating activity. The objective of this study was therefore to optimize the production of PP-*g*-PAA nonmigratory metal chelating active packaging films by manipulating graft conditions of photoinitiator (benzophenone) and acrylic acid. Increasing acrylic acid concentration resulted in an exponential increase in iron chelating activity and manipulating the graft of benzophenone altered the ligand to metal binding ratio. These data suggest that the length of the polymer chains as well as the density of polymer chain graft have a significant impact on the chelating activity of iron chelating films.

EXPERIMENTAL

Materials

Polypropylene (isotactic and pellets) was purchased from Scientific Polymer Products (Ontario, NY). Hydroxylamine hydrochloride, ferrous sulfate heptahydrate (99+%), imidazole (99%), 3-(2-pyridyl)−5,6-diphenyl-1,2,4-triazine-*p,p′*-disulfonic

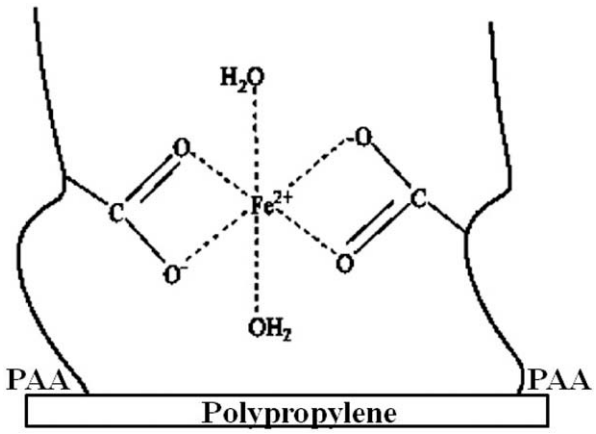

Figure 2. Theoretical binding of ferrous iron by PP-*g*-PAA (adapted with permission from ref. 6. Copyright (2012) American Chemical Society).

Table I. Photoinitiated Graft Polymerization of Acrylic Acid on Polypropylene (PP-*g*-PAA) Reaction Parameters Tested for Study

Role	Compound	Graft condition	Test parameters
Photoinitiator	Benzophenone	Benzophenone concentration (w/w)	5%,[a] 3%, 1%
		Benzophenone graft time	1.5 min,[a] 1 min, 0.5 min
Monomer	Acrylic acid	Acrylic acid concentration (w/w)	30%, 25%,[a] 20%, 15%, 10%
		Acrylic acid graft time	6 min,[a] 4.5 min, 3 min, 1.5 min

[a] Control parameters held constant in optimization experiments.

acid disodium salt hydrate (ferrozine, 98+%), toluidine blue O (TBO), and ethanol (99.5+%) were purchased from Acros Organics (Morris Plains, NJ). Acrylic acid (anhydrous) and benzophenone (99%) were purchased from Sigma-Aldrich (St. Louis, MO). All other chemicals were purchased from Fisher Scientific (Fair Lawn, NJ).

Polypropylene Film Preparation

PP films were prepared as previously reported.[6] PP pellets were cleaned by sequentially sonicating in the following solvents twice for 10 min each rinse: isopropanol, acetone, and deionized water, and then dried over anhydrous calcium sulfate. Clean PP film was prepared on a Carver Laboratory Press (Carver, NJ). The press was set to 160°C, PP pellets were heated on the press for 1 min, and then 9000 lbs of pressure was applied. PP films, average thickness of 387 ± 35 μm, were cut into 2×2 cm^2 pieces and washed using the same method as the PP pellets.

Photoinitiated Graft Surface Modification of PP

Sequential photoinitiated graft polymerization was used to attach poly(acrylic acid) (PAA) to the surface of PP. This method is adapted from previously reported work.[6,17] For this research, concentration and UV exposure time for both the photoinitiator graft and monomer graft and polymerization were examined variables (Table I). The photoinititiator tested was benzophenone and the monomer tested was acrylic acid. Control parameters refer to the grafting conditions for film previously tested for inhibition of lipid oxidation.[6]

Thirty microliters of benzophenone in heptanes was spin coated (WS-400-6NPP, Laurell Technologies, North Wales, PA) onto each side of 2×2 cm^2 PP at 2000 rpm for 10 s. During the spin coating, the spin coater chamber was purged with clean dry air and heptanes were evaporated from the film surface leaving a dried thin layer of benzophenone. The 2×2 cm^2 benzophenone coated PP films were cut into 1×2 cm^2 pieces and then each 1×2 cm^2 piece was placed into a screw top vial and sealed with a septum fitted aluminum cap. The vials were flushed with nitrogen for 5 min and then exposed to UV light (Dymax 5000-EC Series, Torrington, CT) at 365 nm with an average light intensity of 209 ± 4.3 mW cm^{-2}. After benzophenone grafting was completed, the films were washed three times with acetone to remove unreacted benzophenone and then dried at room temperature.

Benzophenone activated PP (PP-BP) films were placed into a screw top vial and 6 mL of acrylic acid in ethanol was added before the vials were sealed with septum fitted aluminum caps. The acrylic acid in ethanol solution in the sealed vials was flushed with nitrogen for 15 min. Nitrogen flushed vials were exposed to UV light to graft and polymerize acrylic acid onto PP-BP. PP-*g*-PAA was rinsed in deionized water for 30 min at room temperature, 60 min at 60°C and then 30 min at room temperature to remove unattached monomer and homopolymer. PP-*g*-PAA was dried overnight over anhydrous calcium sulfate.

Attenuated Total Reflectance/Fourier-Transform Infrared Spectroscopy (ATR-FTIR)

Attenuated total reflectance Fourier transform infrared spectroscopy (ATR-FTIR) was used to confirm the grafting of functional groups on the surface of PP-*g*-PAA. An IRPrestige FTIR Spectrometer (Shimadzu Scientific Instruments, Kyoto, Japan) with a diamond ATR crystal was used to measure the spectrum. Each spectrum was collected under the following parameters: Happ-Genzel function, 32 scans, and 4 cm^{-1} resolution. Spectrum analysis was performed on KnowItAll(R) Informatics System 9.5 (Bio-Rad Laboratories, Informatics Division, Philadelphia, PA) and Sigma Plot 12 (Systat Software, San Jose, CA).

Scanning Electron Microscopy (SEM)

Surface and cross-sectional images of PP-*g*-PAA were taken with JCM-5000 NeoScope (JEOL, Japan) at 10 kV. Cross-sectional samples were prepared by freeze fracturing films under liquid nitrogen. Prior to imaging, samples were mounted on a small aluminum platform with double sided carbon tape and then sputter coated with gold under nitrogen for 3 min. For each treatment, measurements were collected from images taken of two independently prepared replicates.

Contact Angle

Water (HPLC grade deionized water, Fisher Scientific, Fair Lawn, NJ) contact angles of PP-*g*-PAA were measured using a Kruss DSA100 (Hamburg, Germany) equipped with a software controlled direct dosing system (DO3210, Hamburg, Germany) to determine film surface hydrophilicity. Advancing and receding angles were recorded every 0.10 s and calculated using tangent method 2 on DSA software (Hamburg, Germany).

Available Carboxylic Acids Density

TBO dye assay, in which each molecule of dye reversibly binds with carboxylic acids at a 1:1 stoichiometric ratio, was used to quantify surface carboxylic acids as previously described.[5,30,31] Each 1×2 cm^2 film was submerged in 5 mL TBO (0.5 m*M* TBO, pH 10), incubated while shaking at room temperature for 2 h and then rinsed three times in pH 10 deionized water. TBO dye was desorbed from each film in 8 mL 50% acetic acid while

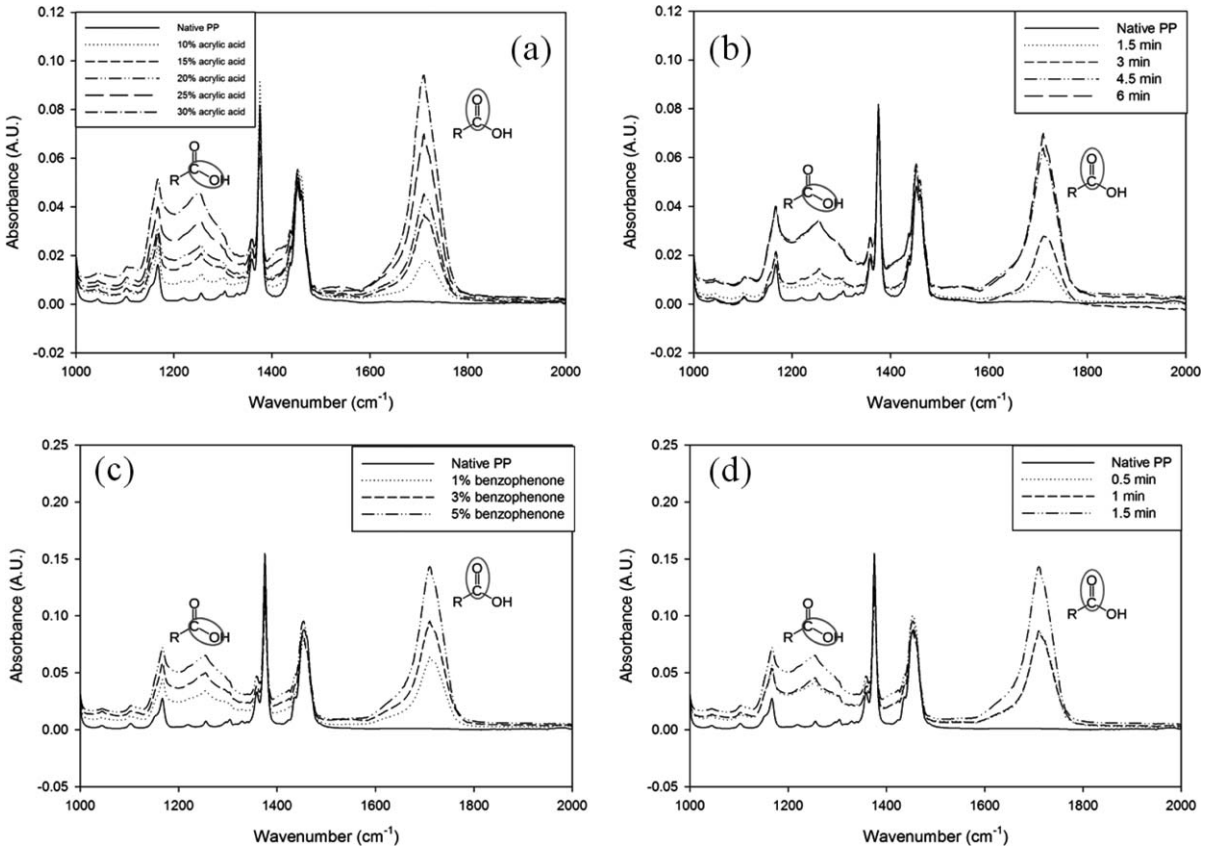

Figure 3. ATR-FTIR of PP-*g*-PAA as affected by (a) acrylic acid concentration, (b) acrylic acid graft time, (c) benzophenone concentration, and (d) benzophenone graft time.

shaking at room temperature for 15 min. The absorbance of TBO dye in 50% acetic acid was measured at 633 nm to quantify surface carboxylic acids by comparison to a standard curve of TBO in 50% acetic acid.

Ferrous Iron Chelating Activity

Iron chelating activity of PP-*g*-PAA was determined by measuring the density of ferrous iron bound to PP-*g*-PAA at pH 5.0 (pH value at which PP-*g*-PAA was previously shown to exhibit optimal ferrous iron chelation).[5,6] In this method, the amount of chelated ferrous iron is released from the film and quantified by colorimetric reaction with ferrozine reagent. Each treatment was submerged in 20 mL of ferrous iron solution (1 m*M* ferrous sulfate heptahydrate in 0.05*M* sodium acetate/imidazole, pH 5.0) and rotated at room temperature for 30 min to attach iron to films and then rinsed three times in deionized water. Ferrous iron was released from the films by incubating each 1 $\times$ 2 cm^2 film with 3 mL of releasing agent (0.1 g/mL hydroxylamine hydrochloride and 0.05 g/mL trichloroacetic acid) while shaking for 2.5 h. After ferrous iron was released from the film, 0.5 mL releasing agent (containing released ferrous iron) was added to 0.5 mL ferrozine solution (9.0 m*M* ferrozine in 50 m*M* HEPES, pH 7.0) and incubated while shaking for 1 h at room temperature. The absorbance of ferrozine reacted releasing agent was measured at 562 nm to quantify ferrous iron chelating activity by comparison to a standard curve of ferrous iron in releasing agent.

Statistical Analysis

All measurements were conducted in at least quadruplicate. Results are expressed at mean $\pm$ standard deviation. For each graft condition examined, a one way ANOVA and Pearson correlation coefficient were calculated using GraphPad Prism 6.0 (La Jolla, CA). Means were separated using a Tukey's post hoc test ($P < 0.05$).

RESULTS AND DISCUSSION

Surface Chemistry

The ATR-FTIR spectra of native PP and PP-*g*-PAA films as affected by acrylic acid concentration, acrylic acid graft time, benzophenone concentration, and benzophenone graft time are shown in Figure 3. ATR-FTIR is a rapid technique for surface chemistry characterization that quantifies specific bonds within a few microns of a substrates surface.[32] In the spectra shown, the narrow absorbance at 1700–1725 cm^{-1} and the broad absorbance at 1211–1320 cm^{-1} illustrate the C═O bond and the C—O bond, respectively, of the carboxylic acids in the PAA graft. Absorbance characteristics of carboxylic acids are not present in the spectra of native PP.

As the acrylic acid concentration and acrylic acid graft time increases, the intensity of absorbance characteristics of carboxylic acid, 1211–1320 cm^{-1} and 1700–1725 cm^{-1}, increases [Figure 3(a,b)]. The acrylic acid graft times of 4.5 and 6 min have similar absorbance intensities, indicating that the graft of PAA

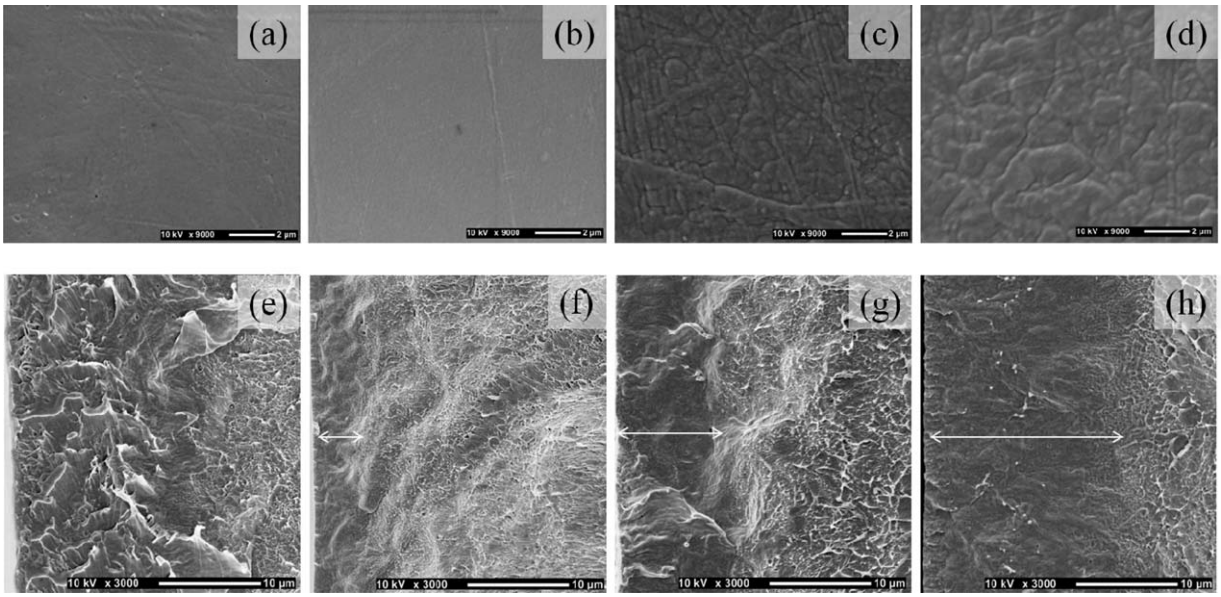

Figure 4. SEM analysis of surface (9000x) of (a) native PP, (b) PP-*g*-PAA (10% acrylic acid), (c) PP-*g*-PAA (control parameters), (d) PP-*g*-PAA (30% acrylic acid) and cross-section (3000x) of (e) native PP, (f) PP-*g*-PAA (10% acrylic acid), (g) PP-*g*-PAA (control parameters), and (h) PP-*g*-PAA (30% acrylic acid). On cross-section images, arrows indicate approximate thickness of PAA graft layer, with the left side being the surface of the grafted film.

may not significantly increase at graft times higher than 4.5 min. As the benzophenone concentration and benzophenone graft time increases, the intensity of carboxylic acid absorbance increases as well [Figure 3(c,d)]. However, it is important to note that contrary to the acrylic acid concentration and graft time treatments, this increase in carboxylic acid absorbance intensity does not correlate with the available carboxylic acids surface density (see "Ligand to Metal Binding" section). None of the treatments contained significantly less available carboxylic acids than the highest benzophenone concentration and graft time tested. Given that ATR-FTIR only measures the first few microns of a substrate's surface and the thickness of the graft layer is >6 μm as measured by SEM (see "Surface and Cross-Section Morphology" section), the decrease peak intensity at lower benzophenone concentrations and graft times suggests a decreased PAA chain graft density. Since PAA chains may only polymerize from benzophenone grafted on PP, lower benzophenone graft would theoretically yield a lower PAA chain graft density.

Surface and Cross-Section Morphology

To determine the effect of PAA graft on the morphology of PP films, surface and cross-section SEM images of the following representative treatments were taken: native PP, 10% acrylic acid (low PAA graft), 25% acrylic acid (control parameters), and 30% acrylic acid (high PAA graft) (Figure 4). Native PP exhibited a relatively smooth surface with a uniform cross-section. Under low PAA graft conditions (10% acrylic acid), there were no noticeable changes in the surface morphology compared with native PP, however a small layer of PAA (6.23 ± 0.94 μm) was present in the cross-section image. Control (25% acrylic acid) and high PAA graft (30% acrylic acid) films exhibited surface cracking and thicker PAA graft layers of 11.2 ± 0.83 μm and 17.6 ± 2.3 μm, respectively. Grafting of poly(acrylic acid) to PP has been previously reported to increase surface cracking and roughness and may be caused by shrinkage of grafted PAA chains under dry conditions.[6,29] Although the interface between the PAA graft layer and PP is not well defined, it is clear that an increase in PAA graft yielded an increased thickness of the PAA graft layer.

Surface Hydrophilicity

Surface hydrophilicity of native PP and PP-*g*-PAA films was determined by measuring advancing and receding angles via water contact angle analysis. Grafting of benzophenone alone (no subsequent PAA grafting) had no significant impact on the advancing and receding angles of native PP. It has been previously reported that surface modification of PP with poly(acrylic acid) improved its surface wettability due to the introduction of hydrophilic carboxylic acids functional groups.[29] All of the PP-*g*-PAA modified films were hydrophilic (advancing and receding contact angle $< 80°$) (see Supporting Information Table S1). Although decreasing the graft of acrylic acid and benzophenone resulted in decreased surface wettability (i.e.: higher advancing water contact angle) of PP-*g*-PAA when compared to control parameters (25% acrylic acid, 6 min acrylic acid graft, 5% benzophenone, 1.5 min benzophenone graft), PP-*g*-PAA films remained hydrophilic compared with native PP films.

Ligand to Metal Binding

The influence of manipulating grafting parameters on the functional properties of the resulting PP-*g*-PAA films was quantified by measuring the number of available carboxylic acids on the films surface using the TBO dye assay and the ferrous iron chelating activity as quantified by the ferrozine assay, described above. The ratio of available carboxylic acids density to iron chelating activity was calculated as the ligand to metal binding ratio. The influence of acrylic acid and benzophenone graft conditions on ligand to metal binding ratio are described below.

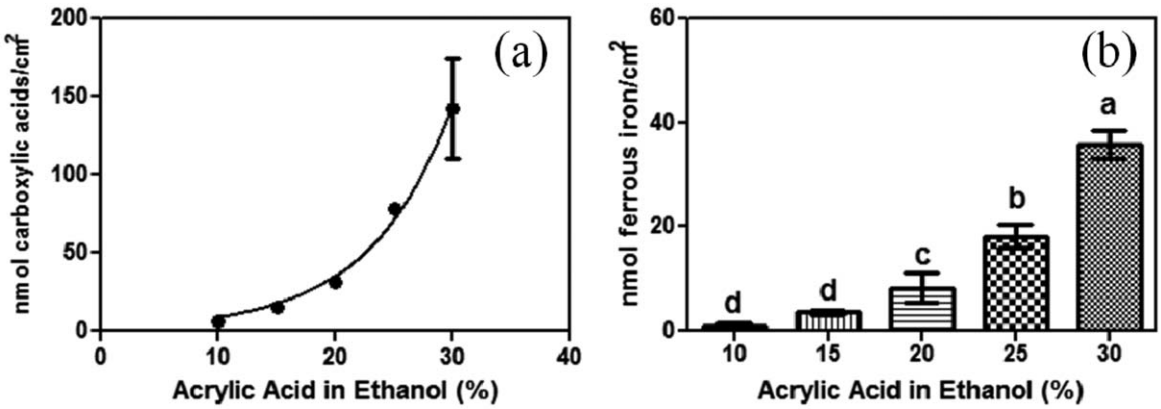

Figure 5. Effect of acrylic acid concentration on (a) available carboxylic acids density and (b) ferrous iron chelating activity. Values are means ± standard deviations ($n = 4$). Letters denote significant differences ($P < 0.05$).

Acrylic Acid Graft Conditions. The effect of acrylic acid concentration on available carboxylic acids density and iron chelating activity is reported in Figure 5. Standard deviations for acrylic acid concentrations ranging from 10 to 25% were less than ±3.5 and therefore are not visible in Figure 5(a). Increasing acrylic acid concentration produced an exponential-like increase in available carboxylic acids on PP-*g*-PAA surface. This increase in carboxylic acids was proportional to the increase in iron chelating activity, with a maximum carboxylic acids density of 143 ± 32 nmol per cm^2 and iron chelating activity of 35.8 ± 2.8 nmol Fe^{2+} per cm^2 at 30% AA. For every 5% increase in acrylic acid concentration, the available carboxylic acids and iron chelating activity roughly doubled. However, at acrylic acid concentrations above 25%, limited solubility and increases in solution polymerization impacted the consistency of graft polymerization, as noted by the larger standard deviation at 30% acrylic acid; therefore, concentrations higher than 30% were not investigated. Figure 6 shows the effect of acrylic acid graft time on available carboxylic acids density and iron chelating activity. As the acrylic acid graft time increased, the available carboxylic acids density increased, approaching a plateau of 77.7 ± 3.5 nmol per cm^2 at 6 min acrylic acid graft times longer than 6 min caused acrylic acid in ethanol solution to leak out of vials due to pressure build up, therefore longer graft times were not investigated. In agreement with the acrylic acid concentration data, the increase in carboxylic acids was proportional to the increase in iron chelating activity. The Pearson correlation coefficient of available carboxylic acids and iron chelating activity for all acrylic acid graft conditions was 0.996 ($P < 0.05$), suggesting that these two measurements are highly correlated. The 4.5 and 6 min graft times did not have significantly different iron chelating activities, 16.4 ± 1.8 nmol Fe^{2+} per cm^2 at 4.5 min and 18.1 ± 2.2 nmol Fe^{2+} per cm^2 at 6 min. This observation corresponds with the similarities in the
ATR-FTIR spectra of 4.5 and 6 min graft time [Figure 3(b)].

Benzophenone Graft Conditions. The effect of benzophenone concentration on available carboxylic acids density and iron chelating activity is shown in Figure 7. There is no distinct trend that correlates benzophenone concentration with available carboxylic acids, but rather it appears that an optimum amount of carboxylic acids, 84.0 ± 15 nmol per cm^2, was grafted at 3% benzophenone. The control parameter (5% benzophenone) exhibited the lowest iron chelating activity, while decreasing the benzophenone concentration to 3% more than doubled the iron chelating activity (45.4 ± 5.9 nmol Fe^{2+} per cm^2 at 3% benzophenone). Figure 8 shows the effect of benzophenone graft time on available carboxylic acids density and iron chelating activity.

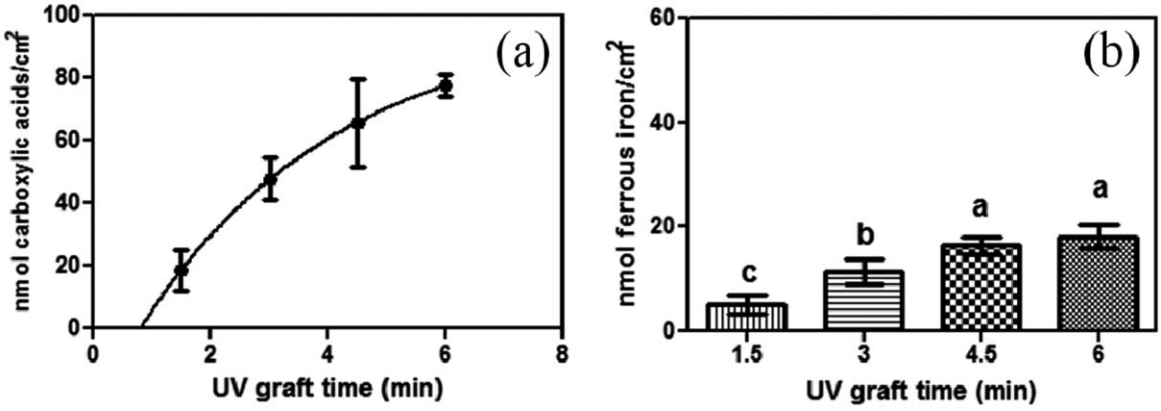

Figure 6. Effect of acrylic acid graft time on (a) available carboxylic acids density and (b) ferrous iron chelating activity. Values are means ± standard deviations ($n = 4$). Letters denote significant differences ($P < 0.05$).

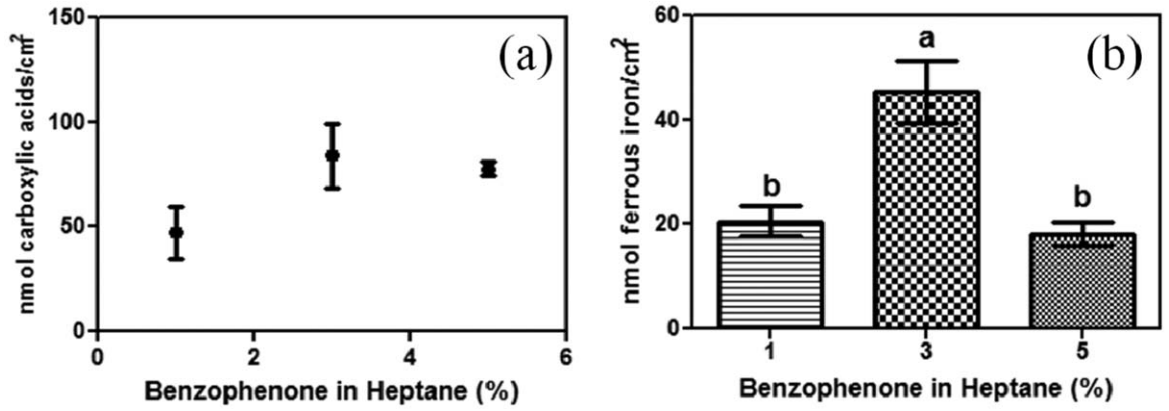

Figure 7. Effect of benzophenone concentration on (a) available carboxylic acids density and (b) ferrous iron chelating activity. Values are means ± standard deviations ($n = 4$). Letters denote significant differences ($P < 0.05$).

Again, there was no clear trend that correlates benzophenone concentration with available carboxylic acids, but rather that an optimum carboxylic acids density of 103 ± 11 nmol per $cm^2$was grafted at 1.0 min benzophenone graft. The control parameter (1.5 min benzophenone graft) exhibited the lowest iron chelating activity, while lower benzophenone graft times exhibited up to almost double of the iron chelating activity, 41.6 ± 2.9 nmol Fe^{2+} per cm^2 at 1.0 min and 29.1 ± 4.7 nmol Fe^{2+} per cm^2 at 0.5 min. Unlike changes to the acrylic acid graft parameters, adjusting the benzophenone graft parameters did not yield proportional increases in the available carboxylic acids and iron chelating activity. The Pearson correlation coefficient of available carboxylic acids and iron chelating activity for all benzophenone graft conditions was 0.625 ($P = 0.185$), suggesting that these two measurements are not highly correlated.

To demonstrate the effect of benzophenone graft conditions on iron chelating activity, the ligand to metal binding ratio for all treatments was calculated and reported in Table II. Reducing benzophenone graft density below control parameter (5% benzophenone and 1.5 min graft time) decreased ligand (carboxylic acid) to metal (Fe^{2+}) ratio from ~4–5 to ~2–2.5. Given that acrylic acid will only polymerize from benzophenone grafted on PP, these data suggest that the density of PAA grafted chains may impact the ligand to metal binding ratio of PP-*g*-PAA. It is hypothesized that higher density PAA grafted chains may exhibit increased apparent ligand to metal binding ratio due to reduced chain flexibility caused by chain crosslinking. PAA chain crosslinking may be initiated by chain transfer reactions or tertiary carbon radicals induced by UV light exposure.[28] More closely packed PAA chains may be more susceptible to these types of reactions. Further experimentation to verify this hypothesis by directly quantifying the effect of crosslinking reactions on chelating activity of polymer chains is required to draw conclusions.

Optimization of PP-g-PAA. The preceding data on the effect of PP-*g*-PAA graft parameters suggest that adjusting control parameters to increase acrylic acid concentration and decreasing graft of benzophenone should yield PP-*g*-PAA with high iron chelating activity. To test this hypothesis, PP-*g*-PAA films were produced under the following parameters 5% benzophenone, 1.0 min benzophenone graft, 30% acrylic acid, and 6.0 min acrylic acid graft. The concentration of BP in solution was not adjusted to optimum conditions (3% BP) because of the effect of reduced solution viscosity of the homogeneity of spin coating. This set of parameters yielded a PP-*g*-PAA film with a carboxylic acids density of 167 ± 31 nmol per cm^2 and iron chelating activity of 76.8 ± 10 nmol Fe^{2+} per cm^2. As predicted by grafting trends, increasing the acrylic acid concentration of the 1.0 min benzophenone graft parameter by 5% roughly

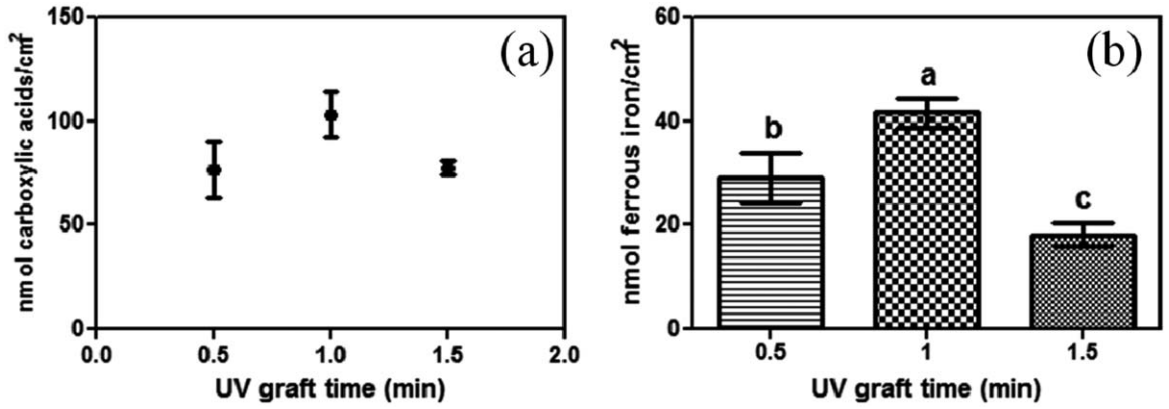

Figure 8. Effect of BP graft time on (a) available carboxylic acids density and (b) ferrous iron chelating activity. Values are means ± standard deviations ($n = 4$). Letters denote significant differences ($P < 0.05$).

Table II. Ligand (COOH) to Metal (Fe^{2+}) Binding Ratio for all Experimental Treatments. Values are means ± standard deviations (n=4). Letters denote significant differences ($p<0.05$).

Graft condition	Test parameters	Ligand to metal binding ratio
Control parameters		$4.30 \pm 0.56^{a,b}$
Benzophenone concentration	3%	1.85 ± 0.42^{b}
	1%	2.30 ± 0.68^{b}
Benzophenone graft time	1 min	$2.48 \pm 0.32^{a,b}$
	0.5 min	$2.63 \pm 0.63^{a,b}$
Acrylic acid concentration	30%	$3.98 \pm 0.94^{a,b}$
	20%	$3.93 \pm 1.39^{a,b}$
	15%	$4.38 \pm 0.81^{a,b}$
	10%	5.42 ± 1.63^{a}
Acrylic acid graft time	4.5 min	$3.99 \pm 0.95^{a,b}$
	3 min	$5.12 \pm 2.29^{a,b}$
	1.5 min	$3.65 \pm 1.83^{a,b}$

doubled available carboxylic acids density and iron chelating activity.

CONCLUSIONS

Herein, we report the effect of adjusting photoinitiated graft polymerization conditions on the surface chemistry and iron chelating activity of PP-*g*-PAA films that have previously demonstrated inhibition of lipid oxidation in an oil-in-water emulsion.[6] Graft chain length and density, manipulated by changing acrylic acid and benzophenone graft conditions, significantly influenced the chelating activity of PP-*g*-PAA both in terms of overall iron binding capacity as well as ligand to metal binding ratio. High chelating activity may be obtained with longer graft chain length (higher acrylic acid graft) and lower graft chain density (lower benzophenone graft) to ensure high amounts of available carboxylic acids and adequate chain flexibility. Such ability to tailor the iron chelating activity of PP-*g*-PAA enables the ability to adapt functional characteristics of chelating polymer materials for specific applications in active packaging for food and consumer products, water purification, and chelation therapy.

ACKNOWLEDGMENTS

The authors acknowledge the Peter Salmon Graduate Fellowship (Department of Food Science, UMass Amherst) and Northeast Alliance Fellowship for their support. This work was supported by the United States Department of Agriculture National Institute of Food and Agriculture (USDA NIFA) competitive grants program. This work was supported, in part, by UMass through the CVIP Technology Development Fund.

REFERENCES

1. Frankel, E. N. *J. Sci. Food Agr.* **1991**, *54*, 495.
2. McClements, D.; Decker, E. *J. Food Sci.* **2000**, *65*, 1270.
3. Pokorný, J. *Eur. J. Lipid Sci. Tech.* **2007**, *109*, 629.
4. Tian, F.; Decker, E. A.; Goddard, J. M. *Food Funct.* **2013**, *4*, 669.
5. Tian, F.; Decker, E. A.; Goddard, J. M. *J. Agric. Food Chem.* **2012**, *60*, 2046.
6. Tian, F.; Decker, E. A.; Goddard, J. M. *J. Agric. Food Chem.* **2012**, *60*, 7710.
7. Koontz, J. *Inform (a magazine published by AOCS)* **2012**, *23*, 598.
8. Goddard, J. M.; Hotchkiss, J. *Prog. Polym. Sci.* **2007**, *32*, 698.
9. Barish, J. A.; Goddard, J. M. *J. Food Sci.* **2011**, *76*, E586.
10. Mahoney, K. W.; Talbert, J. N.; Goddard, J. M. *J. Appl. Polym. Sci.* **2013**, *127*, 1203.
11. Bastarrachea, L. J.; Peleg, M.; McLandsborough, L. A.; Goddard, J. M. *J. Food Eng.* **2013**, *117*, 58.
12. Soares, N.; Hotchkiss, J. *J. Food Sci.* **1998**, *63*, 61.
13. Ozdemir, M.; Yurteri, C. U.; Sadikoglu, H. *Crit. Rev. Food Sci.* **1999**, *39*, 457.
14. Desmet, T.; Morent, R.; Geyter, N. D.; Leys, C.; Schacht, E.; Dubruel, P. *Biomacromolecules* **2009**, *10*, 2351.
15. Deng, J.; Wang, L.; Liu, L.; Yang, W. *Prog. Polym. Sci.* **2009**, *34*, 156.
16. Chan, C.-M.; Ko, T.-M.; Hiraoka, H. *Surf. Sci. Rep.* **1996**, *24*, 1.
17. Ma, H.; Davis, R. H.; Bowman, C. N. *Macromolecules* **2000**, *33*, 331.
18. Rånby, B. *Int. J. Adhes. Adhes.***1999**, *19*, 337.
19. Mohd Yusof, A. H.; Ulbricht, M. *J. Membr. Sci.* **2008**, *311*, 294.
20. Ulbricht, M.; Yang, H. *Chem. Mater.* **2005**, *17*, 2622.
21. Yu, H.-Y.; Xu, Z.-K.; Yang, Q.; Hu, M.-X.; Wang, S.-Y. *J. Membr. Sci.* **2006**, *281*, 658.
22. Ma, H.; Davis, R. H.; Bowman, C. N. *Polymer* **2001**, *42*, 8333.
23. Ulbricht, M. *React. Funct. Polym.* **1996**, *31*, 165.
24. Himstedt, H. H.; Marshall, K. M.; Wickramasinghe, S. R. *J. Membr. Sci.* **2011**, *366*, 373.
25. Mansourpanah, Y.; Habili, E. M. *J. Membr. Sci.* **2001**, *430*, 158.
26. Seman, A.; Khayet, M.; Bin Ali, Z.; Hilal, N. *J. Membr. Sci.* **2010**, *355*, 133.
27. Costamagna, V.; Wunderlin, D.; Larrañaga, M.; Mondragon, I.; Strumia, M. *J. Appl. Polym. Sci.* **2006**, *102*, 2254.
28. Costamagna, V.; Strumia, M.; López-González, M.; Riande, E. *J. Polym. Sci. Part B: Polym. Phys.* **2007**, *45*, 2421.
29. Fasce, L.; Costamagna, V.; Pettarin, V.; Strumia, M.; Frontini, P. *Expr. Polym. Lett.* **2008**, *2*, 779.
30. Uchida, E.; Uyama, Y.; Ikada, Y. *Langmuir* **1993**, *9*, 1121.
31. Kang, E.; Tan, K.; Kato, K.; Uyama, Y.; Ikada, Y. *Macromolecules* **1996**, *29*, 6872.
32. Mirabella, F. M. In Internal Reflection Spectroscopy: Theory and Applications; Mirabella, F. M., Ed.; Marcel Dekker, Inc: New York, **1993**; Chapter *2*, pp 17–52.